JOURNAL OF COMPUTATIONAL PHYSICS 18, 1–20 (1975)

Optimal Particle-Mesh Algorithms

J. W. EASTWOOD

Computer Science Department, University of Reading, Reading, Berkshire, England

Received June 10, 1974; revised December 2, 1974

Optimal particle-mesh algorithms are regarded as those which, for a given computational cost, best represent the physics relevant to the evolution of a computer experiment. A method to determine for arbitrary interparticle force laws a best combination of charge assignment and potential solvers in both momentum and energy conserving schemes is presented. Explicit expressions for the errors in forces and harmonic amplitudes together with expressions for influence functions which minimize those errors are given. A comparison of optimized versions of the common energy and momentum conserving schemes is in Section III, and it is shown how the results of the comparison may be used in deciding which scheme to use for some particular purpose. The application of the error minimizing method to P^3M schemes for ionic systems and to collisionless plasmas is discussed in Sections IV and V, respectively. In Section VI, it is shown how the method may be used to obtain finite difference equations for collisionless plasma simulations.

I. INTRODUCTION

In setting up a particle-mesh code to simulate a many body system, we are confronted with a wide range of possible charge sharing, field solving, and force interpolation schemes and with the limited size and speed of computers. Inevitably a compromise must be made between the accuracy of the representation of the physical system and computational cost. Apriori knowledge of scale lengths and of the phenomena we wish to study gives us guidance as to how coarse our model may be. This in turn may be translated into specifying how closely the mesh calculated force must correspond to the reference force law relevant to the problem in hand. Accordingly, the criterion used in this paper for deciding the optimal algorithm is that the best scheme is that which most economically models the correct force law to within the accuracy required for realistic results.

The objective of the work reported in this paper was to find a systematic method for designing and evaluating particle-mesh algorithms for arbitrary force laws. The basis of the method, namely, quantifying the force in terms of harmonic amplitudes and minimizing the errors in the force by making compensating errors in the potential, is presented in Section II. It is shown in Section III how such

questions as "Are energy conserving schemes better than momentum conserving schemes.·" and "Is CIC more cost effective than NGP.·" may be answered. The application of the method to formulating P^3M algorithms [1] for dense ionic systems is illustrated in Section IV; there it is shown how optimal combinations of charge weighting functions, influence function, cutoff radius and number of particles per cell may be found. Section V contains a discussion of the relevance of the method to collisionless plasmas. Section VI illustrates how optimal finite difference approximations to the field equations may be found and indicates the relationship to the Poisson solvers obtained using Lewis' variational method [2, 3].

II. Errors in the Mesh Calculated Force

We shall consider two classes of force calculating schemes, the so called "momentum conserving schemes" and "energy conserving schemes" [4, 5]. For simplicity, we shall restrict ourselves to 1-dimensional examples; the generalization to higher dimensions is straightforward apart from the additional consideration of potential differencing.

Following Langdon [4, 5, 6] we may write the mesh calculated force F between two charges of charge q in a periodic system as a fourier series: For momentum conserving schemes

$$F(x, \bar{x}) = \frac{q^2}{\epsilon_0 NH^2} \sum_{k=-\infty}^{\infty} \sum_{n=-\infty}^{\infty} \hat{U}_k \hat{d}_k \hat{U}_{-k_n} e^{-inK_g(\bar{x}-(x/2))} e^{iKx}, \tag{1}$$

and for energy conserving schemes,

$$F(x, \bar{x}) = \frac{q^2}{\epsilon_0 NH^2} \sum_{k=-\infty}^{\infty} \sum_{n=-\infty}^{\infty} -iK\hat{U}_k \hat{G}_k \hat{U}_{-k_n} e^{-iK_g n(\bar{x}-(x/2))} e^{iKx}. \tag{2}$$

The notation used in (1) and (2) is as follows. x and $\bar{x}$ are the particles separation and mean position w.r.t. the mesh. Integers p, k and n label configuration space values, harmonic amplitudes, and aliases [23], respectively. $L = NH$ is the period length, where N is the number of mesh points in one period, and H is the cell width. x_p is an integral number of cell widths:

$$x_p = pH. \tag{3}$$

K and K_g are wavenumbers:

$$K = 2\pi k/L, \tag{4}$$

$$K_g = 2\pi/H. \tag{5}$$

$\hat{U}_k$ and $\hat{d}_k$, $\hat{G}_k$ are harmonic amplitudes of the charge weighting function, the mesh electric field Green's function, and the mesh potential Green's function, respectively.

$$\hat{U}_k = \frac{\hat{W}_k}{H} = \frac{1}{H}\int_L W(x)\, e^{-iKx}\, dx, \tag{6}$$

$$\hat{d}_k = H \sum_{p=0}^{N-1} d_p e^{-iKx_p}. \tag{7}$$

The methods of determining the forces implicit in (1) and (2) are computationally inexpensive means of approximating the reference force law

$$R(x) = \frac{q^2}{\epsilon_0 NH^2} \sum_{k=-\infty}^{\infty} \hat{R}_k e^{iKx} \tag{8}$$

Thus, a quantitative measure of the quality of a particular scheme is given by the mean-squared deviation of the mesh calculated forces, F, from R:

$$Q = \frac{1}{LH}\int_L dx \int_H d\bar{x}(F(x,\bar{x}) - R(x))^2 \tag{9}$$

$$= P + Z. \tag{10}$$

P is the mean-squared deviation of the mesh calculated force from the displacement averaged mesh force

$$P = \frac{1}{LH}\int_L dx \int_H d\bar{x}(F(x,\bar{x}) - \langle F(x,\bar{x})\rangle_{\bar{x}})^2, \tag{11}$$

$$\langle F(x,\bar{x})\rangle_{\bar{x}} = \frac{1}{H}\int_H d\bar{x}\, F(x,\bar{x}). \tag{12}$$

Z is the mean-squared deviation of the displacement averaged mesh force $\langle F(x,\bar{x})\rangle_{\bar{x}}$, from the reference force.

(a) *Momentum Conserving Schemes*

Substituting (1) and (8) into (9) and (11) and performing the integrations gives

$$Q = \left[\frac{q^2}{\epsilon_0 NH^2}\right]^2 \sum_{k=0}^{N-1} \left\{ |\hat{d}_k|^2 \left[\sum_n |\hat{U}_{k_n}|^2\right]^2 + \sum_n |\hat{R}_{k_n}|^2 - 2\hat{d}_{-k} \sum_n |\hat{U}_{k_n}|^2 \hat{R}_{k_n} \right\}, \tag{13}$$

and

$$P = \left[\frac{q^2}{\epsilon_0 NH^2}\right]^2 \sum_{k=0}^{N-1} |\hat{d}_k|^2 \left\{ \left[\sum_n |\hat{U}_{k_n}|^2\right]^2 - \sum_n |\hat{U}_{k_n}|^4 \right\}. \tag{14}$$

There are three factors in (13) controlling the magnitude of Q; the aliasing of the reference force, the aliasing of the charge weighting function, and the form of the influence function $\hat{d}_k$. The first of these factors arises because, at best, the mesh can handle only as many harmonics as there are mesh points. Under conditions for physically relevant simulations, the undersampled harmonics of the reference force (wavenumbers $> \pi/H$) are unimportant, and consequently the arbitrary reference force in (13) may, for practical purposes, be replaced by its band limited approximation.

For $\hat{R}_k$ band limited, i.e., $\hat{R}_k \equiv O \forall \mid k \mid \geqslant N/2$,

$$Q = \left[\frac{q^2}{\epsilon_0 NH^2}\right]^2 2 \sum_{k=0}^{(N/2)-1} \left\{ \mid \hat{d}_k \mid^2 \left[\sum_n \mid \hat{U}_{k_n} \mid^2\right]^2 + \mid \hat{R}_k \mid^2 - 2\hat{d}_{-k} \mid \hat{U}_k \mid^2 \hat{R}_k \right\}. \quad (15)$$

The dominance of the principal term in the alias sums in (15) may be made progressively greater by using higher-order (and hence more costly) charge assignment schemes. However, the higher-order schemes attenuate both the adequately sampled and undersampled harmonics, with the result that Q may be larger for higher-order schemes. To offset this effect we may build compensating errors into $\hat{d}_k$:

$$Q = Q^* \text{ is minimum when } (\partial Q/\partial \hat{d}_k) = O \forall k \in [1, (N/2) - 1]$$

giving an optimum $\hat{d}_k$ for a band limited reference force

$$\hat{d}_k = \mid \hat{U}_k \mid^2 \hat{R}_k \Big/ \left| \sum_n \mid \hat{U}_{k_n} \mid^2 \right|^2, \quad (16)$$

and

$$Q^* = \left[\frac{q^2}{\epsilon_0 NH^2}\right]^2 2 \sum_{k=1}^{(N/2)-1} \mid \hat{R}_k \mid^2 \left\{ 1 - \left(\mid \hat{U}_k \mid^4 \Big/ \left| \sum \mid \hat{U}_{k_n} \mid^2 \right|^2 \right) \right\}. \quad (17)$$

(b) *Energy Conserving Schemes*

The evaluation of Q, P and $\hat{G}_k$ for the energy conserving schemes follow in exactly the same manner as for the momentum conserving schemes. For a band limited reference force we have

$$Q = \left(\frac{q^2}{\epsilon_0 NH^2}\right)^2 \sum_k \left\{ \hat{G}_k^2 \left(\sum_n \mid \hat{U}_{k_n} \mid^2\right)\left(\sum_n K_n^2 \mid \hat{U}_{k_n} \mid^2\right) + \mid \hat{R}_k \mid^2 - 2i\hat{G}_k K \mid \hat{U}_k \mid^2 \hat{R}_k \right\}, \quad (18)$$

$$P = \left(\frac{q^2}{\epsilon_0 NH^2}\right)^2 \sum_k \hat{G}_k^2 \left\{ \left(\sum_n \mid \hat{U}_{k_n} \mid^2\right)\left(\sum_n K_n^2 \mid \hat{U}_{k_n} \mid^2\right) - \sum_n K_n^2 \mid \hat{U}_{k_n} \mid^4 \right\}, \quad (19)$$

optimal $\hat{G}_k$

$$\hat{G}_k = iK \mid \hat{U}_k \mid^2 \hat{R}_k \Big/ \Big(\sum_n \mid \hat{U}_{k_n} \mid^2\Big)\Big(\sum_n K_n^2 \mid \hat{U}_{k_n} \mid^2\Big), \tag{20}$$

$$Q^* = \Big(\frac{q^2}{\epsilon_0 N H^2}\Big)^2 2 \sum_{k=0}^{(N/2)-1} \mid \hat{R}_k \mid^2 \Big(1 - \frac{K^2 \mid \hat{U}_k \mid^4}{(\sum_n \mid \hat{U}_{k_n} \mid^2)(\sum_n K_n^2 \mid \hat{U}_{k_n} \mid^2)}\Big). \tag{21}$$

III. A Comparison of Q-Minimized Schemes

Three useful quantities for measuring how well an algorithm represents various wavelengths are $Q_k^\dagger$, $P_k^\dagger$, $Z_k^\dagger$. $Q_k^\dagger$ is the fractional mean-squared deviation of the mesh calculated amplitude of the kth harmonic from its true value, $P_k^\dagger$ is that part of $Q_k^\dagger$ due to the fluctuation of the interparticle force under mesh displacements, and $Z_k^\dagger$ is the part of $Q_k^\dagger$ due to deviation of the displacement averaged mesh force from its true value. From Eqs. (17) and (21) we have

$$Q_k^\dagger = 1 - \Big(\mid \hat{U}_k \mid^4 \Big/ \Big| \sum \mid \hat{U}_{k_n} \mid^2 \Big|^2\Big) \tag{22}$$

for momentum conserving schemes, and

$$Q_k^\dagger = 1 - \Big[K^2 \mid \hat{U}_k \mid^4 \Big/ \Big(\sum_n \mid \hat{U}_{k_n} \mid^2\Big)\Big(\sum_n K_n \mid \hat{U}_{k_n} \mid^2\Big)\Big] \tag{23}$$

for energy conserving schemes. Corresponding expressions for $P_k^\dagger$ and $Z_k^\dagger$ may be obtained using Eqs. (10), (14), (16), (19), and (20). Note that the quantities $Q_k^\dagger$, $P_k^\dagger$, and $Z_k^\dagger$ are independent of both the form of the force law and the number of mesh points used.

The results of the numerical evaluation of $Q_k^\dagger$, $P_k^\dagger$, and $Z_k^\dagger$ for some Q-minimized schemes are summarized in Figs. 1–3. Schemes considered are momentum conserving ones ($\hat{d}_k$ defined by Eq. (16)) using NGP, CIC, and TSC charge weights [7–10] and energy conserving ones ($\hat{G}_k$ defined by (20)) using linear interpolation (ELI) and quadratic splines (EQS), respectively [2, 5, 11, 18].

Figure 1 shows the percentage r.m.s. errors in the harmonic amplitudes as a function of wavenumber. Bearing in mind that these curves give the *minimum possible errors* for each of the charge-sharing/force-interpolation combinations and are *independent of the interparticle force law*, they provide an unbiased comparison between the various schemes. As is to be expected, the curves indicate that smaller wavenumbers are better represented than larger ones, and that the curves are ordered in cost/quality, with both energy and momentum conserving schemes

showing comparable errors. The breakdown of the errors in Figs. 2 and 3 show that, except for very short wavelengths, fluctuations are the major contributor to $(Q_k^{\dagger})^{1/2}$, with the ratio of $(P_k^{\dagger})^{1/2}$ to $(Z_k^{\dagger})^{1/2}$ increasing with the order of the scheme,

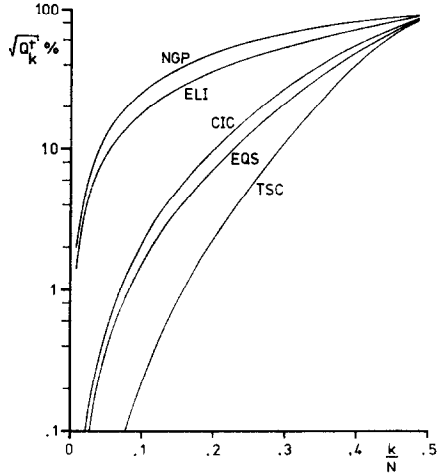

FIG. 1. The minimum r.m.s. percentage deviation of the kth harmonic of the mesh calculated force from the kth harmonic of the reference force as a function of wavenumber for an arbitrary band limited force law. NGP, ELI, CIC, EQS, and TSC refer to the charge assignment/force interpolation schemes relevant to each curve.

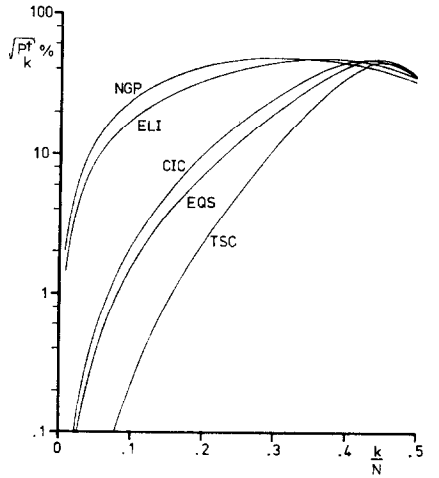

FIG. 2. The r.m.s. percentage deviation of the kth harmonic of the mesh calculated force from the kth harmonic of the mesh displacement averaged force vs wavenumber for the influence function employed to obtain the curves in Fig. 1. The curves are labeled as in Fig. 1.

and decreasing with increasing wavenumbers. Note the relatively small difference in errors between NGP and ELI and between CIC and EQS schemes, whereas they show quite a large difference in cost per particle per timestep.

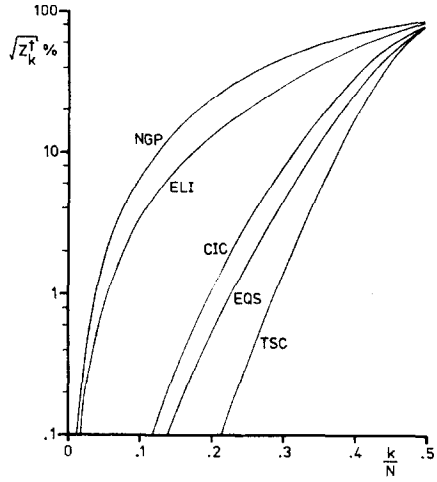

FIG. 3. The r.m.s. percentage deviation of the kth harmonic of the displacement averaged mesh force from the kth harmonic of the reference force as a function of wavenumber for the cases shown in Figs. 1 and 2.

The value of the method and results presented in this and the previous section are that (i) the method provides a prescription which gives the best influence functions (see Eqs. (16) and (20)) to go with a particular charge sharing scheme for both energy and momentum conserving schemes (cf. Lewis' approach for energy conserving schemes [2, 3]) and (ii) the results enable the most cost effective scheme for a particular role to be chosen. To illustrate the second point, let us consider an example:

Assume that we want to simulate a system of length $L = 100\lambda_D$ (λ_D = Debye length), and that we require the error in all wavelengths greater than $2\lambda_D$ to be less than 10%. Which of the five schemes discussed above is the cheapest in terms of cost per particle per timestep?

Drawing a line parallel to the abcissa through $(Q_k^\dagger)^{1/2} = 10\,\%$ in Fig. 1, we obtain the maximum $k/N = (k/N)\,|_{10\%}$ for the 10% condition to be met. Equating the wavelength corresponding to $(k/N)\,|_{10\%}$ to $2\lambda_D$ gives the minimum number of mesh points for which the criterion can be met:

$$N = 50/(k/N)\,|_{10\%}\,. \tag{24}$$

Assuming that two FFT are used in determining the potential or field as appropriate from the charge, then the operation count, T_i, for scheme i will be approximately of the form

$$T_i = \alpha_i m + \beta N_i \log_2 N_i . \tag{25}$$

α_i is a measure of the number of operations per particle per timestep in the charge sharing, force interpolation and time-stepping parts of the calculation loop, m is the number of particles, and N_i is the number of mesh points. The breakeven number of particles, m, between scheme i and scheme j is given when $T_i = T_j$:

$$m = -\beta[N_i \log_2 N_i - N_j \log_2 N_j]/(\alpha_i - \alpha_j). \tag{26}$$

Using the real arithmetic operations count to estimate α and β, we have for TSC–EQS, ESQ–CIC, CIC–ELI, and ELI–NGP, $\Delta\alpha = \alpha_i - \alpha_j = 5$, 6, 3, 4, respectively, and $\beta = 5$ [7]. Inserting these values into (26), and using (24) and Fig. 1 to obtain N, we find the ranges of m over which each particular scheme is most economical:

NGP: $m > 8000$

ELI: NONE

CIC: $325 < m < 8000$

EQS: NONE

TSC: $m < 325$

Nowhere do the energy conserving cases prove economical. The requirements on the particle numbers for the system to behave like a Vlasov fluid i.e., $m\lambda_D/L \gg 1$ [6, 12, 13, 14] precludes the regime where TSC is cheapest, and the fact that NGP requires at least five times the number of mesh points that CIC needs (from (24) and Fig. 1) militates against the large number of particles required for NGP to be most economical. For this example, Q-minimized CIC with $N = 256$ is the most economial. Additional economy and an increase of heating and collision times may be achieved by setting $\hat{d}_k$ to zero for the poorly represented short wavelengths ($\lambda < 2\lambda_D$ for this case) [15, 16].

IV. Q-Minimized P^3M Schemes

Until recently, dense ionic systems were simulated using the simple, but computationally expensive, direct particle–particle sum to obtain interparticle forces. A new technique suggested by Hockney [1], which reduces the force calculation operation count from dependence on the square of the number of particles to a

linear dependence on the number of particles, is to express the interparticle forces forces as the sum of the mesh part, E, and the direct sum part $F_{\text{s.r.}}$:

$$F = E + F_{\text{s.r.}}, \tag{27}$$

where the short range direct sum contribution is over particles of separations less than some cutoff value a. The scalelength in systems for which P^3M is appropriate is of the order of ion separations, the particles are identified as molecules and the strong short range forces are such that the potential and kinetic energies are comparable. Consequently, we require a mesh force, E, which accurately models the total force, F, for separations greater than a and goes smoothly to zero for small particle separations. Let us now use the simple case of a Coulombic force in one dimension to show how the Q-minimizing method may be advantageously employing in finding a suitable algorithm for determining E:

The reference force, $R(x)$, for the mesh calculated force, E, may, by Gauss' Law, be regarded as the force between finite sized particles of width $a/2$ [12, 13]. The harmonic of R are

$$\hat{R}_k = (-iH/K) \mid \hat{S}_k \mid^2, \tag{28}$$

where $\hat{S}_k$ is the kth harmonic of the decomposition of the density distribution of the charge in the particle:

$$\hat{S}_k = \int_L dx\, S(x)\, e^{-iKx}. \tag{29}$$

Note that since $S(x)$ is nonzero only for the finite range $\mid x \mid < a/2$ of x, $\hat{S}_k$ is nonzero for all k, implying that $\hat{R}_k$ is not band limited for the finite sized particle. However, by matching higher and higher derivatives of the force at $\mid x \mid = a$, we obtain progressively faster decays of the amplitudes $\hat{R}_k$ with k:

Specifying continuity of the mesh force, $R(x)$ and its first derivative at $x = a$ gives the "top-hat" shaped cloud (shape S1):

$$S(x) = \begin{cases} \dfrac{1}{a}; & \mid x \mid < a/2, \\ 0; & \text{otherwise}, \end{cases} \tag{30}$$

$$\hat{S}_k = [\sin(Ka/2)]/(Ka/2). \tag{31}$$

Specifying continuity of $R(x)$, $R'(x)$, $R''(x)$, $R'''(x)$ at $x = a$ gives the triangular shaped cloud (shape $S2$)

$$S(x) = \begin{cases} \dfrac{-\mid x \mid + (a/2)}{(a/2)^2}; & \mid x \mid < a/2, \\ 0; & \text{otherwise}, \end{cases} \tag{32}$$

$$\hat{S}_k = [\sin^2(Ka/4)]/(Ka/4)^2. \tag{33}$$

Similarly, progressively higher-order fitting of derivatives yields reference cloud shape Sn:

$$\hat{S}_k = \text{sinc}^n(Ka/2n); \qquad n = 1, 2, 3, 4,.... \tag{34}$$

To obtain the full benefit of the faster decay of $\hat{S}_k$ with k for higher n schemes, greater cutoff radii, a, must be employed to offset the increase of n in the denominator of the argument of the sinc function in (34). Computational cheapness dictates that a shall be as small as possible, so only the small n schemes prove practical.

Results for the $n = 1$ (S1) and $n = 2$ (S2) cloud shapes are presented in Figs. 4 and 5. Reference forces defined by (28), (31), and (32) are used to obtain Q for Q-minimized schemes. The labels NGP, CIC, and TSC again refer to the charge weighting/force interpolation functions, and the curves labeled MIN, the differences between the band limited and exact reference force, give the minimum error that can be achieved in the mesh force. Plotted are $(Q^{\dagger})^{1/2}$, the root mean-squared deviation of the mesh force, E, from the reference force, R, expressed as a percentage of the r.m.s. force between point particles vs the cutoff radius in units of cell widths. Values given are for $N = 128$; for other choices of N, multiply values on the ordinates by $(128/N)^{1/2}$.

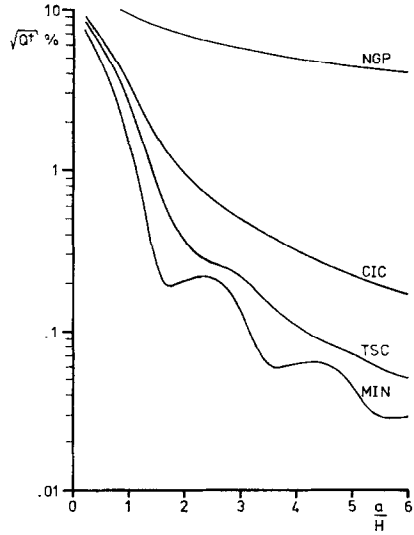

FIG. 4. The minimum r.m.s. deviation $(Q^{\dagger})^{1/2}$, of the mesh calculated force from the top-hat (S1) shaped particle reference force as a function of the cutoff radius. NGP, CIC, TSC refer to the charge assignment/force interpolation scheme. MIN labels the curve arising when a band limited charge assignment scheme is used. The curves shown are for $N = 128$. $(Q^{\dagger})^{1/2}$ is expressed as a percentage of the r.m.s. force between two charged planes.

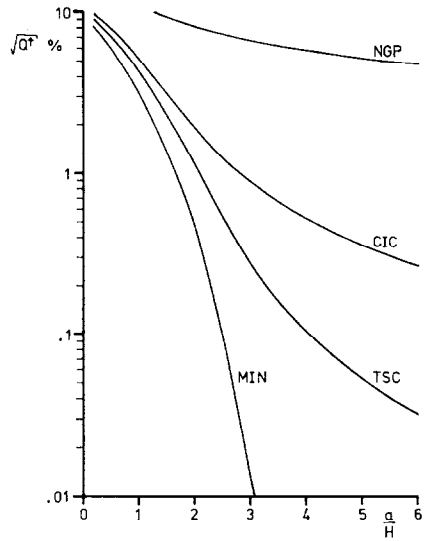

FIG. 5. The minimum r.m.s. deviation, $(Q^\dagger)^{1/2}$, of the mesh calculated force from the triangular shaped particle (S2) reference force as a function of cutoff radius for $N = 128$. Labeling and normalization are the same as for Fig. 4.

Comparing Fig. 4 and 5, we see that the smallest $\text{MIN}(Q^\dagger)^{1/2}$ is given by the S1 reference cloud shape for a/H small, with the crossover to the S2 shape ocurring at $a/H \simeq 2.3$. A similar crossover from S1 to S2 occurs for TSC at $a/H \simeq 4$, although no such changeover appears for NGP and CIC in the range of $(a/H)(<12)$ investigated. Note that for the TSC/S1 example $(Q^\dagger)^{1/2}$ remains within a factor two of the minimum possible value, indicating that no significant gain will be achieved by using higher-order schemes. A larger disparity between the values of $(Q^\dagger)^{1/2}$ for the TSC scheme and the $\text{MIN}(Q^\dagger)^{1/2}$ is apparent for the S2 reference force (Fig. 5). In this case, using higher-order schemes than TSC may prove profitable, especially for $a/H > 4$.

To find the best scheme, we proceed in a similar manner to that illustrated in the previous section. For example, suppose we require a scheme which will give a coulombic interparticle for with an r.m.s. error of less than 0.1 %.

The operation count for the P^3M scheme is of the form

$$T = \alpha m + \beta N \log_2 N + \gamma m r(m/N), \tag{35}$$

where α, β, m, and N are as defined in Section III, $r = a/H$, and γ is the operation count per particle for the short range correction. At the optimum number of particles per cell,

$$(m/N)_{\text{opt}} = [\beta \log_2 N/\gamma r]^{1/2}, \tag{36}$$

the last two terms in (35) are equal, and the operations per particle per timestep is approximately constant:

$$\Gamma = T/m = \alpha + 2[\gamma r\beta \log_2 N]^{1/2}. \tag{37}$$

From Figs. 4 and 5, it is clear that NGP is impractical. The breakeven between CIC and TSC is found by eqating Γ for the two schemes:

$$(r_{\mathrm{CIC}})^{1/2} - (r_{\mathrm{RSC}})^{1/2} = (\alpha_{\mathrm{TSC}} - \alpha_{\mathrm{CIC}})/2[\gamma\beta \log_2 N]^{1/2}. \tag{38}$$

Again using real arithmetic operation counts, we find $\alpha_{\mathrm{TSC}} - \alpha_{\mathrm{CIC}} = 11$, $\beta = 5$, $\gamma \simeq 15$ and, for $N = 128$, $\log_2 N = 7$. Inserting these values into (38), we find that r_{CIC} must be less than 5 in order that CIC be more economical than TSC. It is clear from Figs. 4 and 5 that it is not, indicating that TSC should be used. Finally, we must decide which reference force to use. Both S1 and S2 give $\sim$0.1 % error at $r = a/H = 4$. However, from Fig. 6, we see that fluctuations for the S1 mesh force are less than for S2, and hence S1 is to be preferred for its better energy conservation properties.

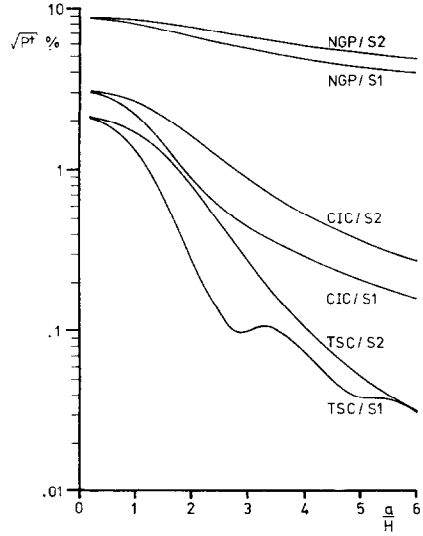

FIG. 6. The r.m.s. deviation of the mesh calculated force from the displacement averaged mesh force expressed as a percentage of the force between two charged planes versus cutoff radius. The curves correspond to the examples of $(Q^t)^{1/2}$ given in Figs. 4 and 5.

We now have all the information required to set up the optimal $1 - D$ P^3M code to give coulombic forces with less than 0.1 % error: TSC charge sharing, the

optimal number of particle per cell (Eq. (36)), an S1 reference force with cutoff radius $a = 4H$, and an influence function given by

$$\hat{d}_k = \left(\sum_{n=-\infty}^{\infty} | \hat{U}_{k_n} |^2 \hat{R}_{k_n} \right) \Big/ \left[\sum_n | \hat{U}_{k_n} |^2 \right]^2, \tag{39}$$

$$= \frac{-iH^2 \cot x \cos^2 x \cos^2 2x[1 - \sin^2 x + (1/5) \sin^4 x + (1/315) \sin^6 x]}{2(1 - \sin^2 x + (2/15) \sin^4 x)^2}, \tag{40}$$

where

$$x = \pi k/N = KH/2. \tag{41}$$

In addition, if FFT are not used to obtain the field from the charge, then (40) may be fourier transformed to give the optimal difference approximation to the field equation.

V. Q-Minimized Plasma Simulations

Collisionless plasma simulations involve a compromise between dispersive properties, collision times and heating times within the constraints of the finite computer resources. The best compromise is that which, for given computational cost, most accurately emulates the behavior of a Vlasov fluid over the spatial and temporal scales of interest. Factors affecting the compromise are (i) the paucity of particles, which enhances collisional effects [14, 17], (ii) the band limiting effect of the mesh, which suppress short wavelengths and reduces collisional effects [6, 12], (iii) undersampling of the density, leading to increased heating rate and modified dispersion [4–7], and (iv) the smoothing effect of interpolation [13].

Fortunately, (i) and (ii) are partially cancelling. Using the most cost effective scheme (cf. Section III) and discarding unimportant wavelengths minimizes the unwanted consequences. Aliasing (point (iii)) can have disastrous effects [19], but provided that the characteristic wavelength, λ, of collective motions in the system is such that $H \ll \lambda \ll L$, the resulting mesh-induced fluctuations of wavelengths of importance are quite small (cf. Fig. 2). The many short wavelengths of little importance to collective behavior present when $H \ll \lambda \ll L$ should be suppressed to improve collision and heating times (see [16] for proof of the benefits of this truncation).

The wavelengths which are retained may be treated using the Q-minimizing method. The dispersion relation for an electrostatic Vlasov plasma is [23]

$$1 = -\frac{\omega_p^2}{K} \int_c \frac{f_0'(v)\, dv}{\omega - Kv}, \tag{42}$$

whereas that for a momentum conserving particle-mesh plasma is [4]

$$1 = -\omega_p^2 \frac{\hat{d}_k}{iH} \int_c f_0'(v)\, dv \sum_n \frac{|\hat{U}_{kn}|^2}{\omega - K_n v}. \tag{43}$$

In the long wavelength limit ($\pi k/N = KH/2 \ll 1$), (43) reduces to

$$1 = -\frac{K\hat{d}_k |\hat{U}_k|^2}{iH} \left\{ \frac{-\omega_p^2}{K} \int_c \frac{f_0'(v)\, dv}{\omega - Kv} + O\left(\left(\frac{\pi k}{N}\right)^{2m+1}\right) \right\}, \tag{44}$$

where

$$m = \begin{cases} 1 & \text{for NGP,} \\ 2 & \text{for CIC,} \\ 3 & \text{for TSC,} \end{cases} \tag{45}$$

(In (44) the leading error term becomes $O((\pi k/N)^{2m+2})$ for a stationary symmetric distribution).

Choosing $\hat{d}_k$ to minimize Q (Eq. (16)) gives

$$-K\hat{d}_k |\hat{U}_k|^2/iH = |\hat{U}_k|^4 \Big/ \left[\sum_n |\hat{U}_{k_n}|^2\right]^2, \tag{46}$$

$$= 1 + O((\pi k/N)^{2m}). \tag{47}$$

Comparing (44) and (47) shows that the leading error is in the influence function for Q-minimized momentum conserving schemes. (Similar results may be obtained for the energy conserving schemes). Better long wavelength dispersion can be obtained by setting

$$\hat{d}_k = -iH(|\hat{U}_k|^2/K). \tag{48}$$

If FFT are used to solve the field equations, then the latter choice, (48), may be advantageous, although the smaller fluctuations (and hence better energy conservation) given by the Q-minimized schemes for marginally poorer dispersion may outweigh any such advantage. Further research is needed to resolve this fine point. Here, it is assumed that Q-minimized schemes are used in view of their wider applicability.

The advantage of Q-minimized schemes over some other plausible schemes is illustrated by Fig. 7. If we assume that the desired response to small amplitude disturbances in the range of wavelengths retained by the computer model is given by (42), then a comparison of different algorithms is provided by the relative deviation of the harmonic amplitudes from the values required by (42). Plotted in Fig. 7 is the percentage r.m.s. errors in the harmonic amplitudes as a function of wavenumber for four 1-dimensional CIC schemes. The labeling of the curves indicates the method of determining the field from the charge.

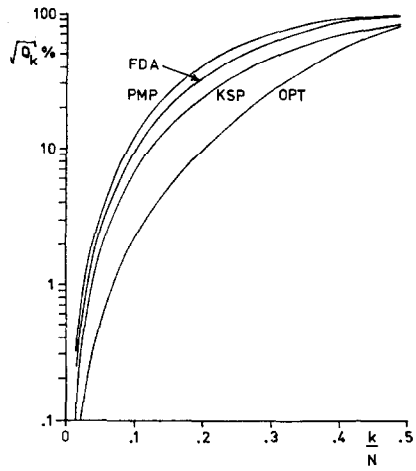

FIG. 7. The r.m.s. percentage deviation of the mesh calculated harmonic amplitudes from the harmonic amplitudes of a coulombic force law for four CIC particle mesh schemes. See text for details of labeling of curves.

(i) The Poor Man's Poisson solver (PMP):

$$\begin{aligned} 2HE_p &= \phi_{p-1} - \phi_{p+1}, \\ \hat{\phi}_k &= \hat{\rho}_k/\epsilon_0 K^2 \end{aligned} \tag{49}$$

(a 1-D analog of the scheme of Boris and Roberts [15]).

(ii) The finite difference approximation (FDA):

$$\begin{aligned} 2HE_p &= \phi_{p-1} - \phi_{p+1}, \\ \phi_{p-1} - 2\phi_p + \phi_{p+1} &= -\rho_p H^2/\epsilon_0 \end{aligned} \tag{50}$$

(a 1-D analog of Birsall and Fuss' scheme [8]).

(iii) Direct k-space solution (KSP):

$$\hat{E}_k = -i\hat{\rho}_k/\epsilon_0 K \tag{51}$$

(cf. the field solution in the dipole approximation scheme [21]).

(iv) The Q-minimized scheme (OPT):

$$\hat{E}_k = \hat{d}_k \hat{\rho}_k/\epsilon_0 H, \tag{52}$$

where $\hat{d}_k$ is given by (16).

The errors built into the influence function, $\hat{d}_k$, by scheme (iv) offset the errors arising in charge sharing and force interpolation to the extent that the overall errors are typically a factor of three smaller than those given by (i)–(iii). Larger improvements are obtained for higher-order charge sharing schemes, as the limiting factor is the relative strengths of the principal modes and aliased modes contributions to harmonic amplitudes.

VI. Finite Difference Equations

In the previous section we saw that Q-minimized schemes enable good dispersive properties to be obtained for long wavelengths, with truncation of k-space (cf. [16]) being used to control collision and heating times. It will now be shown that if we sacrifice the harmonic by harmonic fine tuning available when FFT are used to solve the field equation, then finite difference equations corresponding to Q-minimizing influence functions may be found.

(a) *Momentum Concerving Schemes*

The Q-minimizing influence function for a coulombic force between finite-sized particles is· from (28) and (39),

$$\hat{d}_k = -iH\left(\sum_n |\hat{U}_{k_n}|^2 |\hat{S}_{k_n}|^2 / K_n\right) \Big/ \left[\sum_n |\hat{U}_{k_n}|^2\right]^2, \tag{53}$$

where [5]

$$\begin{aligned} \hat{U}_k &= (\sin(\pi k/N)/\pi k/N)^m, \\ m &= \begin{cases} 1 & \text{for NGP,} \\ 2 & \text{for CIC,} \\ 3 & \text{for TSC.} \end{cases} \end{aligned} \tag{54}$$

Using the identity [20]

$$\frac{d^s}{dx^s}\operatorname{cosec}^2 x = \sum_n \frac{1}{(x+\pi n)^{2+s}} \tag{55}$$

enables (53) to be written in terms of trigonometric functions. The finite difference equations are then obtained by transforming

$$\hat{E}_k = \hat{d}_k \hat{\rho}_k / \epsilon_0 H. \tag{56}$$

For example, the best NGP approximation to the force between point particles ($\hat{S}_k = 1$) is given when

$$\hat{d}_k = (-iH^2/2)\cot(\pi k/N). \tag{57}$$

Finite difference equations corresponding to (57) are

$$\begin{aligned} \phi_{p+1} - 2\phi_p + \phi_{p-1} &= -\rho_p H^2/\epsilon_0 , \\ E_p &= (\phi_{p-1} - \phi_{p+1})/2H. \end{aligned} \tag{58}$$

The influence function (57) gives a multiplying factor in the dispersion relation (44) of

$$-K\hat{d}_k \mid \hat{U}_k \mid^2/iH = 1 + O((\pi k/N)^2). \tag{59}$$

Dispersive properties of the NGP model may be improved at the cost of stronger fluctuations by minimizing Z rather than Q, giving

$$\hat{d}_k = (-iH^2/2)[\cot(\pi k/N)]/[(1 - \tfrac{2}{3}\sin^2(\pi k/N))], \tag{60}$$

and

$$-K\hat{d}_k \mid \hat{U}_k \mid^2/iH = 1 + O((\pi k/N)^4). \tag{61}$$

Smoothing may be introduced by using specific charge shapes in (53). Convenient choices are given by (31) and (33) with a equal to an integral multiple of the cell width, H. The advantages of this procedure are that problems with self forces and nonconservation of momentum are avoided, and that the effect on dispersive properties may be readily evaluated.

(b) *Energy Conserving Schemes*

Finite difference equations which minimize Q or Z, and introduce smoothing may be obtained in the manner indicated above. In particular, the influence function, $\hat{G}_k$, which minimizes Q for the point particle reference force is

$$\hat{G}_k = H \Big/ \sum_n K_n^2 \mid U_{k_n} \mid^2. \tag{62}$$

Equation (62) is identical to Lewis' prescription for the potential solver [5], i.e., Lewis' variation method applied to the approximate Lagrangian is equivalent to minimizing the r.m.s. error in the force. That this should be so may be seen by writing Q for energy conserving schemes in terms of the approximated Lagrangian, **L**, for quasistatic fields:

$$Q = \frac{1}{L}\int_L R^2(x)\, dx - \frac{2}{\epsilon_0 LH}\int_H dx\, \mathbf{L}, \tag{63}$$

where (see (49) in [2])

$$\mathbf{L} = \int_L dx' \left\{\rho\phi_m - \frac{\epsilon_0}{2}\left(\frac{d\phi_m}{dx}\right)^2\right\}. \tag{64}$$

ρ is the (exact) charge density, and ϕ_m is the mesh calculated potential

$$\phi_m(x) = \sum_{p=0}^{N-1} W(x - x_p)\, \phi_p \,.$$

Since the first term in (63) is independent of the mesh potential, applying Hamilton's Principle to (64) gives the same Euler–Lagrange equation, and hence the same Poisson solver, as minimizing Q does.

As noted by Langdon [5], the potential solver specified by (62) does not give the best long wavelength dispersive properties. Minimizing Z to obtain $\hat{G}_k$,

$$\hat{G}_k = \sum_n |\, \hat{U}_{k_n} |^2 \Big/ \sum K_n^2 \,|\, \hat{U}_{k_n} |^4$$

improves the dispersive properties (cf. momentum conserving schemes), but, again, only at the expense of increasing P.

VII. Concluding Remarks

One-dimensional examples have been given in this paper to substantiate the worth of the systematic approach to obtaining good codes. The method is even more valuable in two and three dimensions, where the wider variety of schemes and more severe consequences of computer limitations would otherwise magnify the difficulty of the choice of algorithm. The generalization of the expressions for Q, P, Z, etc., to higher dimensions presents no serious problems. Forces, wavenumbers, and alias numbers are replaced by their relevant vector quantities and sums by double or treble sums as appropriate. Additional factors may be readily included. For example, optimal combinations of Poisson solver and field differencing for momentum conserving schemes may be found by suitably constraining the electric field influence function. Interlaced schemes [24] may be treated by modifying the expression for the mesh calculated force (Eqs. (1) and (2)). Effects of code optimization (such as use of word packing, efficient buffering, integer arithmetic, and machine coding [7, 15, 16, 21]) on the relative economics of the various schemes may be handled by adjusting the coefficients in the timing equations.

The author rejects as inadequate the criterion that if you can find one scheme which is grid insensitive, then it would be best for all purposes. Such a viewpoint, in extremes, would lead to the conclusion that noninteracting particles or meshless systems are best, and, in moderation, may lead to orders of magnitude more computing than is necessary to achieve the desired ends (cf. Section III). An optimal scheme, in the sense of the criterion proposed in this paper, is the one which is

most economical in obtaining less than a given mean-squared deviation from the reference value.

In P^3M calculations, it is clear that minimizing Q gives the physically most desirable result. Harmonic amplitudes which are severely corrupted by aliasing are suppressed in the mesh part of the force, and replaced by adjusting the tabulated short range correction. The overall effect is to accurately and economically represent the prescribed forces between the ions. The role of the reference force in this type of scheme is to provide a systematic method of adjusting the balance between the mesh and short range part of the calculation.

The reference force has a direct physical meaning in the context of collisionless plasma simulations. Landau damping in Vlasov plasmas and band limiting in particle mesh models both have the effect of suppressing short wavelengths, a feature which may be conveniently interpreted by ascribing a finite size to the particles [13]. The intrinsic shape of the finite sized particle is of little relevance provided that it leads to the required physical behavior. A "wide" particle (radius $\gg \lambda_D$) increases collision times [4, 12, 16, 17] at the expense of dispersive properties, and vice versa for "narrow" particles. Changing the reference force alters the balance between dispersive and collisional effects, and allows the effective charge shape to be estimated.

In Section VI, it was shown that the finite sized particle reference force gave smoothing prescriptions for altering the effective particle width (a feature which Lewis could have, but did not, include in his examples [2]). However, if FFT are used to solve the field equations, the greater freedom in the form of the approximate field equations gives the more useful result that long wavelength dispersion and the collision effects can be treated independently. Errors in the harmonic amplitudes of long wavelength are minimized by adjusting the influence function, and collision and heating times are varied by truncating k-space. This approach gives peculiar effective charge shapes, such as the sinc-shaped particle which corresponds to the band limited coulombic reference force, but provides a good description of Vlasov plasmas (the sinc function is defined in [22, Chap. 4]). Again, no one scheme is best for all purposes. For short computations, many harmonics may be retained at the expense of collision and heating times, while for long computations, some of the harmonics may be traded off to reduce the unwanted kinetic effects. Indeed, in the latter case, the effective width of the finite sized particle may be made greater than the Debye length without affecting the collective response of the model to long wavelengths.

ACKNOWLEDGMENT

Financial support was provided by a United Kingdom Atomic Energy Authority extramural contract.

REFERENCES

1. R. W. HOCKNEY, S. P. GOEL, AND J. W. EASTWOOD, *Chem. Phys. Lett.* **21** (1973), 589.
2. H. R. LEWIS, *Meth. Comp. Phys.* **9** (1970), 307.
3. H. R. LEWIS, *J. Computational Phys.* **6** (1970), 136.
4. A. B. LANGDON, *J. Computational Phys.* **6** (1970), 247.
5. A. B. LANGDON, *J. Computational Phys.* **12** (1973), 247.
6. A. B. LANGDON, "Proceedings of the Fourth Annual Conference on the Numerical Simulation of Plasmas," Office of Naval Research Department of the Navy, Arlington, Va., 1970.
7. R. W. HOCKNEY, *Meth. Comp. Phys.* **9** (1970), 136.
8. C. K. BIRDSALL AND D. FUSS, *J. Computational Phys.* **3** (1969), 494.
9. R. L. MORSE, *Meth. Comp. Phys.* **9** (1970), 213.
10. E. W. HOCKNEY, S. P. GOEL, AND J. W. EASTWOOD, *J. Computational Phys.* **14** (1974), 148.
11. O. BUNEMAN, *J. Computational Phys.* **11** (1973), 250.
12. C. K. BIRDSALL, A. B. LANGDON, AND H. OKUDA, *Meth. Comp. Phys.* **9** (1970), 241.
13. A. B. LANGDON AND C. K. BIRDSALL, *Phys. Fluids* **13** (1970), 2115.
14. H. OKUDA AND C. K. BIRDSALL, *Phys. Fluids* **13** (1970), 2123.
15. J. P. BORIS AND K. V. ROBERTS, *J. Computational Phys.* **4** (1969), 4.
16. J. H. ORENS, J. P. BORIS, AND I. HABER, "Proceedings of the Fourth Annual Conference on the Numerical Simulation of Plasmas," Office of Naval Research Department of the Navy, Arlington, Va., 1970.
17. R. W. HOCKNEY, *J. Computational Phys.* **8** (1971), 19.
18. H. R. LEWIS, A. SYKES, AND J. A. WESSON, *J. Computational Phys.* **10** (1972), 85.
19. H. OKUDA, *J. Computational Phys.* **10** (1972), 475.
20. T. J. I'A BROMWICH, "An Introduction to the Theory of Infinite Series," 2nd ed., pg. 216, MacMillan, London, 1965.
21. W. L. KRUER, J. M. DAWSON, AND B. ROSEN, *J. Computational Phys.* **13** (1973), 114.
22. R. BRACEWELL, "The Fourier Transform and its Application," Chap. 10, McGraw–Hill, New York, 1965.
23. T. H. STIX, "The Theory of Plasma Waves," Chap. 7, McGraw–Hill, New York, 1962.
24. L. CHEN, A. B. LANGDON, AND C. K. BIRDSALL, *J. Computational Phys.* **14** (1974), 200.